Preprints of the 21st IFAC World Congress (Virtual)
Berlin, Germany, July 12-17, 2020

Experimental data-driven tumor modeling for chemotherapy ⋆

Dániel András Drexler * **Tamás Ferenci** * **András Füredi** **,*** **Gergely Szakács** **,*** **Levente Kovács** *

* *Physiological Controls Research Center, Research and Innovation Center of Óbuda University, Óbuda University, Hungary (e-mails: {drexler.daniel,ferenci.tamas,levente.kovacs}@nik.uni-obuda.hu).*
** *Institute of Cancer Research, Medical University of Vienna, Austria (e-mails: {andras.furedi,gergely.szakacs}@meduniwien.ac.at).*
*** *Institute of Enzymology, Research Centre for Natural Sciences, Hungary (emails: {furedi.andras,szakas.gergely}@ttk.mta.hu)*

Abstract: Mathematical models of tumor growth in response to chemotherapy are crucial for therapy optimization and outcome. We create a relatively simple tumor growth model describing the antitumor effect of pegylated liposomal doxorubicin (PLD) validated with real experimental data obtained in a genetically engineered mouse model of breast cancer. We use formal reaction kinetics to describe the pathophysiological phenomena using differential equations, and carry out parametric identification based on experiments using a mixed-effect model with stochastic approximation expectation maximization. The model gives a sufficient fit to describe tumor growth and pharmacokinetic data, and a satisfactory fit for the complex case, i.e., tumor response to chemotherapy. The results showed that identification of certain subsystems is easy using experimental data even if it is not specifically designed for identification. However, the identification of the complex pathophysiological phenomena may require experiments specially designed for identification purposes.

Keywords: Model formulation, experiment design; Identification and validation; Pharmacokinetics and drug delivery

1. INTRODUCTION

Mathematical modeling is becoming an increasingly valuable tool for studying therapeutic and chemotherapeutic drug effect in cancer. Several models have been defined in the literature with different complexity, see e.g. the reviews of Altrock et al. (2015) and Jarrett et al. (2018). However, validation is usually restricted to relatively simple model structures, and complex models are not validated with clinical data.

A model of HIV-related non-Hodgkin lyphosomas is given by Aogo and Nyabadza (2018), where the differential equations have eight states and the authors use 42 parameters. They carry out sensitivity analysis and analyse the steady-states of the model. Chakravarty and Dalal (2019) analyse an intracellular drug dynamics model with seven states. They carry out the qualitative analysis of the system and prove the boundedness of the solutions. Paez Chavez et al. (2019) create a model for the effect of chemotherapy on HIV/AIDS-cancer dynamics. They use a model with six states and 22 parameters. They show the boundedness of the solutions, and consider therapy optimization with a fixed amount of drug. They use an impulsive system. Fabian Morales-Delgado et al. (2019) use fractional-order differential equations to describe tumor dynamics. These models are rather complex, and there is no validation using clinical data in the literature.

Murphy et al. (2016) use clinical data to evaluate different tumor dynamics models. They use relatively simple models to model the tumor dynamics; they show that the exponential models and logistic models have the best fits. They use similar measurements we use for the untreated tumor in Subsection 2.2, where we show that the exponential-like model can describe the experimental data. Kühleitner et al. (2019) use untreated tumor growth data to identify a Bertalanffy-Pütter type tumor model, however, this model can not take the effect of drug into consideration.

We propose an impulsive system with four states and nine parameters with mostly linear terms in the differential equations and carry out parametric identification based on experiments in Section 3. The experiments are based on the response of a murine breast cancer model to treatment by pegylated liposomal doxorubicin (PLD or Doxil) as published in Füredi et al. (2017). The experimental results encompass a large time span (between 80 and 250 days) and show rich dynamics of the treated tumor.

⋆ This project has received funding from the European Research Council (ERC) under the European Union's Horizon 2020 research and innovation programme (grant agreement No 679681). The present work has also been supported by the Hungarian National Research, Development and Innovation Office (2018- 2.1.11-T ÉT-SI-2018-00007 and SNN 125739).

Initially, we use the model from Drexler et al. (2017) and Drexler et al. (2019b) with three states and reformulate it to get an impulsive system described in Subsection 2.1. We use measurements carried out on nine mice with breast cancer without treatment to identify the parameters for the tumor growth dynamics in Subsection 2.2. We use pharmacokinetics measurements from three mice without tumor in Subsection 3.1 to identify the pharmacokinetics parameters of the drug. Based on the results, we replace the mixed-order pharmacokinetic model used in Drexler et al. (2017) with a two-compartment pharmacokinetic model, thus increase the number of states by one. Finally, the tumor growth model containing pharmacokinetics and effect of the drug is identified in Subsection 3.2. We use only the experimental results of seven out of 10 mice, where the drug resistance does not seem to be evident based on the measurements. The results show that a relatively simple model can effectively capture the rich dynamics of the treated tumor in a large time span.

2. TUMOR GROWTH MODEL

2.1 The original model and the impulsive model

The differential equations describing the tumor growth used in (Drexler et al. (2019a)) are

$$\dot{x}_1 = (a-n)\,x_1 - b\frac{x_1 x_3}{ED_{50}+x_3} \tag{1}$$

$$\dot{x}_2 = nx_1 - wx_2 + b\frac{x_1 x_3}{ED_{50}+x_3} \tag{2}$$

$$\dot{x}_3 = -c\frac{x_3}{K_B+x_3} - b_\kappa\frac{x_1 x_3}{ED_{50}+x_3} + u, \tag{3}$$

where x_1 is the time function of the living tumor volume [mm^3], x_2 is the time function of the dead tumor volume [mm^3] and x_3 is the time function of the drug level [mg/kg], while u is the time function of the drug input [mg/kg/day].The output of the system is the total tumor volume, i.e., $y = x_1 + x_2$, which is the measured variable in the experiments.

The terms in the differential equations can be explained with formal reaction kinetics analogy (Tóth et al. (2018)), by supposing that X_1, X_2 and X_3 are fictive species corresponding to the living tumor volume, dead tumor volume and drug level. The fictive reaction steps

$$X_1 \xrightarrow{a} 2\,X_1 \tag{4}$$

$$X_1 \xrightarrow{n} X_2 \tag{5}$$

$$X_1 + X_3 \xrightarrow{b} X_2 \tag{6}$$

$$X_3 \xrightarrow{c} O, \tag{7}$$

describe the tumor proliferation (4), tumor necrosis without drug (5), effect of the drug (6) and clearance of the drug (7). The first two equations are considered with mass-action kinetics resulting in linear terms in the differential equations, while the last two equations are considered with Michaelis-Menten kinetics resulting in Hill functions in the differential equations having extra parameters ED_{50} and K_B as Michaelis-Menten constants of reactions (6) and (7), respectively. Hill functions are used widely in biological models to describe saturated effects, see e.g. the work of Ionescu (2018).

The system dynamics is defined by the differential equations (1)-(3), supposing that the input u is a continuous function of time. However, in practice, the input is an injection, thus the dynamical model should be described by differential inclusions, i.e., generalization of differential equations with discontinuous right-hand side (Perestyuk et al. (2011)). Thus, we remove u from the differential equations, and consider the input as discontinuity in the drug level x_3 in the following way.

Let the time of injections be denoted by t_i, with $i = 1, 2, \ldots$, and the dose of injection at time instant t_i be u_i. Then the system dynamics is described by the differential equations (1)-(3) with $u = 0$ on the intervals $[0, t_1]$, $[t_1, t_2]$, $\ldots$,$[t_i, t_{i+1}], \ldots$ and in the time instants t_i, $i = 1, 2, \ldots$ we have

$$x_3(t_i^+) = x_3(t_i^-) + u_i. \tag{8}$$

2.2 Tumor growth dynamics

The tumor growth dynamics without treatment is described by the formal reaction kinetics equations (4)-(5), considered with mass-action kinetics (Érdi and Tóth (1989)), resulting in

$$\dot{x}_1 = (a-n)\,x_1 \tag{9}$$

$$\dot{x}_2 = nx_1 - wx_2. \tag{10}$$

We use measurements with untreated tumor to identify the parameters a, n and w. The measurements were carried out on nine mice (SAL1-SAL9). We suppose that initially $x_2(0) = 0$ mm^3, and estimate $x_1(0)$. The identification is carried out by converting the system of equations into a mixed-effect model and then applying stochastic approximation Expectation-Maximization (SAEM) algorithm as in (Drexler et al. (2019a)).

The results of the identification are shown in Fig. 1. For each mouse, the magenta circles show the measurements, while the blue circles show the estimated values based on the differential equations (9)-(10) and the estimated parameters and initial values. The measured and estimated values are interpolated linearly only for visualization purposes. The results show that a good fit can be achieved with the differential equations.

The estimated parameters for the population mean are shown in Table 1 along with the between-subject variation, standard errors and confidence intervals. The confidence interval of the parameter w shows that the available measurements are not sufficient to estimate this parameter accurately. This deficiency will be corrected later in the identification phase based on the treated cases.

3. EFFECT OF CHEMOTHERAPY

3.1 Pharmacokinetics of PLD

The pharmacokinetics of the drug is defined by (7) in the original model in Drexler et al. (2019a), which results in the Hill function

$$\dot{x}_3 = -c\frac{x_3}{K_B+x_3}. \tag{11}$$

We carried out parametric identification based on measurements with three mice (MouseA, MouseB and MouseC),

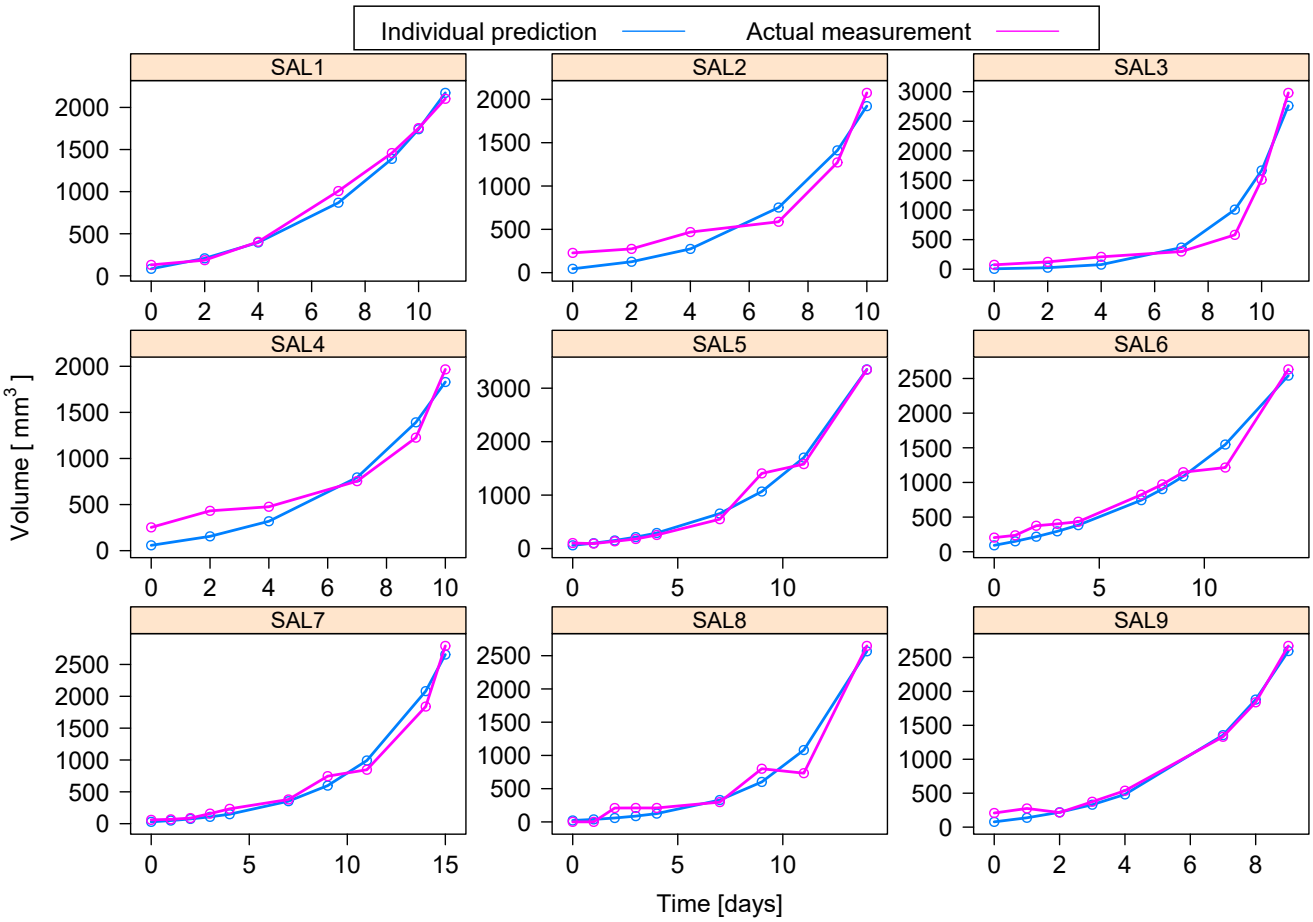

Fig. 1. Untreated tumor growth in nine mice

Parameter	Est.	SE	%RSE	Back-transformed(95%CI)	BSV(CV%)
Log a	-0.437	0.294	67.2	0.646 (0.363, 1.15)	11.7
Log n	-0.982	0.514	52.3	0.374 (0.137, 1.03)	15.7
Log w	-17.5	$6.85{\cdot}10^{4}$	$3.91{\cdot}10^{5}$	$2.42{\cdot}10^{\ 8}$ $(0, \infty)$	108.
Log x10	3.74	0.395	10.6	41.9 (19.3, 91)	99.6
Additive error	158			158	

Table 1. Numerical results for the untreated model. (SE: standard error, RSE: relative standard error, BSV: between-subject variation.)

where healthy mice got only one injection (8 mg/kg), and the serum levels [ng/ml] were measured at certain time instants [minutes]. The measurements are shown by green dots in Fig. 2.

The initial value $x_3(0)$ was considered as an identified parameter. The identification was carried out using the same methodology as previously. The results are shown by the blue curves in Fig. 2. The blue curves are not shown after about 4000 minutes since the values were close to zero and plotting them would hinder the visualization. The fit is not satisfactory, so we modified the pharmacokinetics model to a two-compartment model.

Let X_3 denote the fictive species corresponding to the drug level in the central compartment, and X_4 be the fictive species corresponding to the drug level in the peripheral compartment. The fictive chemical equations describing the pharmacokinetics are

$$X_3 \underset{k_2}{\overset{k_1}{\rightleftarrows}} X_4 \tag{12}$$

$$X_3 \xrightarrow{c} O. \tag{13}$$

These equations are considered with mass-action kinetics to get

$$\dot{x}_3 = -(c + k_1)x_3 + k_2 x_4 \tag{14}$$

$$\dot{x}_4 = k_1 x_3 - k_2 x_4. \tag{15}$$

Here x_3 and x_4 are serum levels, and they have the dimension [ng/ml]. During the parametric identification, $x_3(0)$ is an identified parameter, while we suppose that $x_4(0) = 0$. The results after the identification are shown by the magenta curves in Fig. 2, which shows that this model has significantly better fit, thus we use the two-compartment model for the final version of the model used in the next subsection.

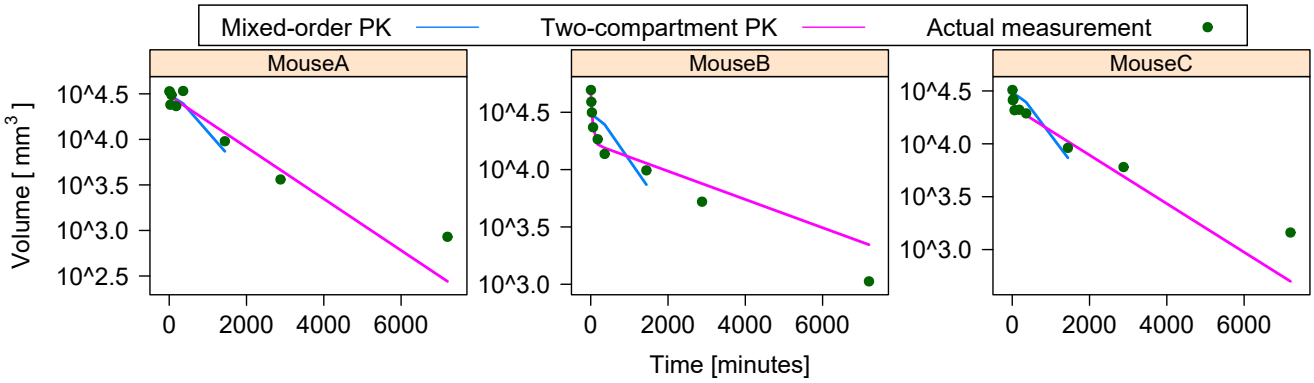

Fig. 2. Serum levels of PLD in three different mice

The identified parameters for the mean population are shown in Table 2, along with the standard errors, confidence intervals and between-subject variation. The between-subject variations show that the parameters c and k_1 are very stable, i.e., almost the same for all the mice.

3.2 Treated case with PLD

The model used to describe the tumor growth and the effect of PLD is the combination of the equations (4)-(6) and (12)-(13), which results in the differential equations

$$\dot{x}_1 = (a-n)\,x_1 - b\frac{x_1 x_3}{ED_{50}+x_3} \tag{16}$$

$$\dot{x}_2 = nx_1 + b\frac{x_1 x_3}{ED_{50}+x_3} - wx_2 \tag{17}$$

$$\dot{x}_3 = -(c+k_1)\,x_3 + k_2 x_4 - b_k\frac{x_1 x_3}{ED_{50}+x_3} \tag{18}$$

$$\dot{x}_4 = k_1 x_3 - k_2 x_4 \tag{19}$$

describing the dynamics in the intervals $[0, t_1]$, $[t_1, t_2]$, ..., $[t_i, t_{i+1}]$,... for $i = 1, 2, \ldots$. The states correspond to the living tumor volume [mm^3], necrotic tumor volume [mm^3], drug level in the central compartment [mg/kg] and drug level in the peripheral compartment [mg/kg], respectively. The injections u_i at time instants t_i are considered as given in (8), thus the drug is injected into the central compartment. The output of the model, which is the measured tumor volume in the experiment, is the total tumor volume, i.e., $y = x_1 + x_2$.

The parametric identification was carried out using measurements where the mice recieved 8 mg/kg dose of PLD at certain time instants according to the protocol described in Füredi et al. (2017). The experiment was carried out with 10 mice (PLD1–PLD10); we used only those results (seven mice) where we supposed that the mice did not acquire resistance against the drug (Fig. 3). The identification was carried out using the same methodology, the initial value $x_1(0)$ was estimated as a parameter, while the other states were supposed to be zero initially. For the initial estimation of the parameters a, n, w we have used the values from Table 1, while for the initial estimation of the parameters c, k_1, k_2 we used the values from Table 2. Note that the unit of the parameters in Table 2 are given in [1/min], while the unit of the parameters in the current model is [1/day], thus the parameters from Table 2 had to be multiplied by 1440 to convert from [1/min] to [1/day]. The first identification results showed that the parameter b_k is close to zero, so for having better convergence, we supposed during the identification that $b_k = 0$.

The result of the identification is shown in Fig. 3. The simulated values based on the model and the identified parameters are the blue circles, while the measured values are the magenta circles. The values are interpolated linearly for visualization purposes. The black arrows indicate the time of injections. The results show that the model is able to follow the trends. Note that the measurements are carried out by calipers, measuring only the length and width of the tumor, and the volume is approximated with a formula, which can result in large measurement errors. This implies that based on caliper measurements, it is hard to decide if the measured results for PLD5 oscillate around the estimated values due to the measurement error, or due to the dynamics of the original system. This can be clarified using more accurate measurements (e.g., using small animal MRI) in the future.

The identified parameter values for the mean population are shown in Table 3. The parameter with the largest between-subject variation is the median effective dose (ED_{50}), which is the parameter responsible for the order of magnitude of the dose during therapy optimization Drexler and Kovács (2019). If the therapy optimization is done offline, i.e., the feedback is not available during therapy, and the protocol has to be generated using virtual patients, then, provided the large between-subject variability, the virtual patient with largest ED_{50} should be chosen for therapy generation.

4. DISCUSSION AND CONCLUSIONS

We proposed a tumor growth model incorporating the effect and pharmacokinetics of PLD. The model has four states and nine parameters, and most of the terms in the differential equations are linear. The model is formulated using formal reaction kinetics analogy, which helps the interpretation of the terms and parameters of the equations. The results of the identification provided good fits for the untreated case and the pure pharmacokinetics measurements, however, for the treated case, the fits show diverse performance. The fits are good for some mice, however, for some mice, the performance of the identified model needs improvement. The performance is limited due to the fact that we can only measure the sum of the first

Parameter	Est.	SE	%RSE	Back-transformed (95% CI)	BSV (CV%)
Log c	-7.12	0.161	2.26	0.000809 (0.00059, 0.00111)	0.262
Log k1	-4.13	0.295	7.13	0.0161 (0.00902, 0.0286)	0.759
Log k2	-3.63	0.61	16.8	0.0265 (0.00802, 0.0876)	109.
Log x30	10.6	0.109	1.03	$4.02{\cdot}10^4$ ($3.24{\cdot}10^4$, $4.97{\cdot}10^4$)	16.4
Additive error	$3.13{\cdot}10^3$			$3.13{\cdot}10^3$	

Table 2. Numerical results for the well-fitting two-comparment pharmacokinetic model. (SE: standard error, RSE: relative standard error, BSV: between-subject variation.)

Parameter	Est.	SE	%RSE	Back-transformed (95 %CI)	BSV (CV%)
Log a	-2.08	0.207	9.94	0.125 (0.0834, 0.187)	47.6
Log n	-8.07	4.81	59.5	0.000312 ($2.53{\cdot}10^{-8}$, 3.85)	178.
Log b	-0.801	0.296	37	0.449 (0.251, 0.802)	59.9
Log ED50	-7.48	3.18	42.5	0.000562 ($1.11{\cdot}10^{-6}$, 0.285)	2480.
Log w	-3.29	0.42	12.7	0.0371 (0.0163, 0.0845)	143.
Log c	-0.211	0.216	103	0.81 (0.53, 1.24)	36.2
Log k1	1.91	1.31	68.6	6.78 (0.518, 88.8)	82.0
Log k2	4.2	0.971	23.1	66.7 (9.95, 447)	113.
Log x10	3.6	0.426	11.8	36.7 (15.9, 84.6)	125.
Additive error	109			109	

Table 3. Numerical results for the treated model. (SE: standard error, RSE: relative standard error, BSV: between-subject variation.)

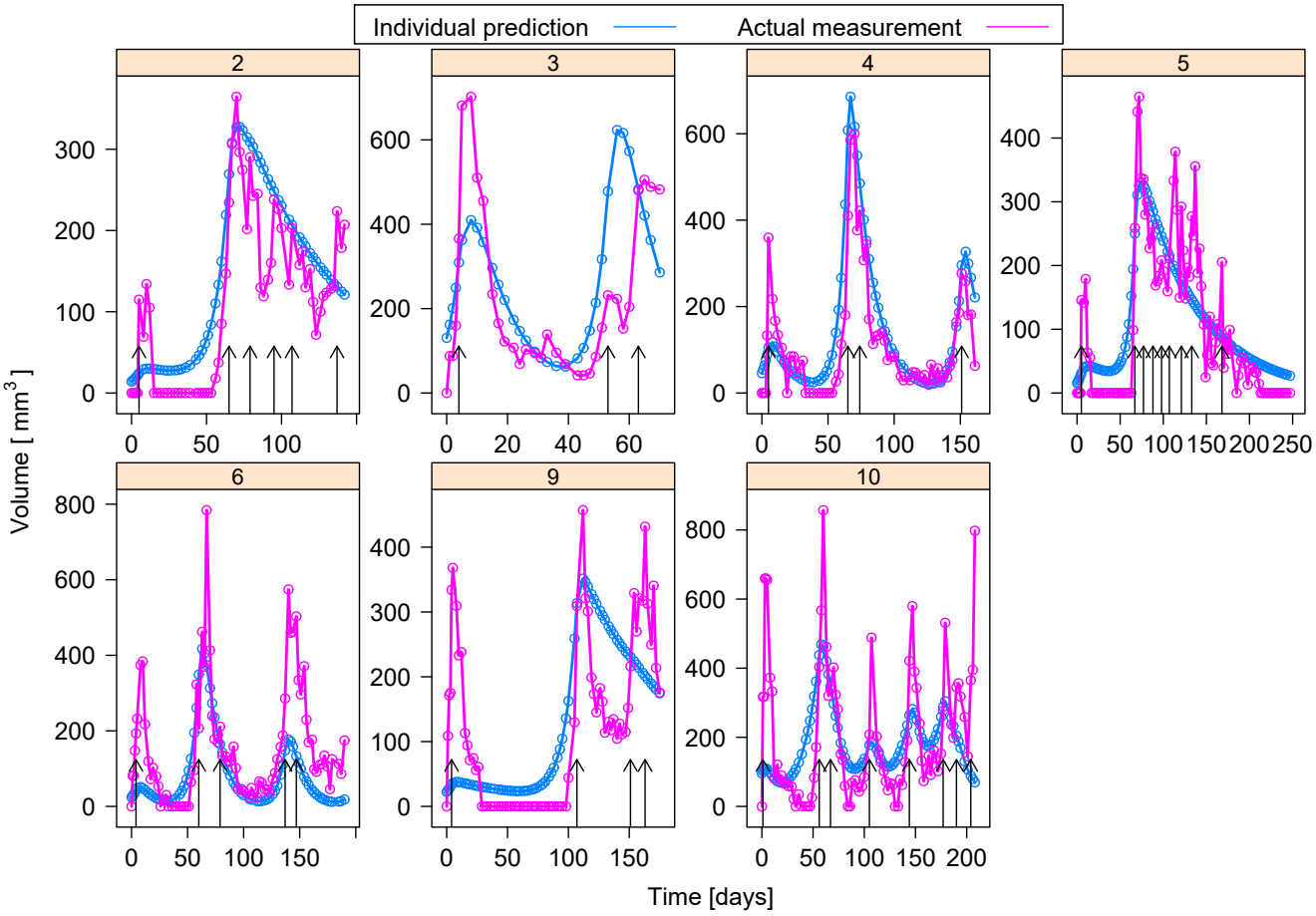

Fig. 3. Treated tumor growth using PLD in seven mice

two states. The performance can be increased by having measurements from more states of the system, which is subject to further research.

The identification of such model is not a straightforward task. The high number of parameters (relative to the available observations) makes the results sensitive to the choice of starting values. (I.e., the algorithm often converges to a local optimum.) To counter this, we employed several different countermeasures. First, we increased both the burn-in and the number of EM steps in the SAEM algorithm. Much more importantly, we employed a hier-

archical strategy: we run submodels with fewer number of parameters and less equations (e.g., purely pharmacokinetic model and the untreated tumor growth), extracted the final estimated values and used them as starting values in the more complex model for the respective parameters. We also re-started SAEM after the fitting was done to make sure that no further convergence happens. Overall, this strategy resulted in a much better fit than the naive estimation.

The model can be developed further by adding additional physiological phenomena. The experimental results show that after the first injection, the tumor is almost totally eliminated (see cases 2,4, 5, 6 and 9 in Fig. 3), and in these cases the tumor remains in a rested state for a certain time. In this state, tumor proliferation has different speed than in the normal phase, which is not considered in the model. This results in bad fit for the intervals after the first treatment where the measured volume is zero. This is a limitation of the current model and can be improved by changing the tumor proliferation rate when the tumor volumes are small.

When the tumor grows back after the first successful treatment, its physiological parameters (proliferation rate, sensitivity to the drug, etc) may be different then in the initial phase. In the current form of the model, the parameters are supposed to be constant, thus this phenomenon is not taken into consideration. A possible direction for improvement is to incorporate the effect of treatment on the model parameters, which could be an alternative to incorporate the acquired drug resistane into the model.

REFERENCES

Altrock, P.M., Liu, L.L., and Michor, F. (2015). The mathematics of cancer: integrating quantitative models. *Nature Reviews. Cancer*, 15(12), 730–745. doi: 10.1038/nrc4029.

Aogo, R. and Nyabadza, F. (2018). Modelling the dynamics of HIV-related non-Hodgkin lymphomas in the presence of HIV treatment and chemotherapy. *Mathematical Methods in the Applied Sciences*, 41(18), 8385–8406. doi:10.1002/mma.4566.

Chakravarty, K. and Dalal, D.C. (2019). Stability analysis of drug dynamics model: A mathematical approach. *International Journal of Biomathematics*, 12(4), 1950043. doi:10.1142/S1793524519500438.

Drexler, D.A. and Kovács, L. (2019). Optimization of impulsive discrete-time tumor chemotherapy. In *Proceedings of the 2019 IEEE 1st International Conference on Societal Automation*.

Drexler, D.A., Ferenci, T., Lovrics, A., and Kovács, L. (2019a). Modeling of tumor growth incorporating the effect of pegylated liposomal doxorubicin. In *Proceedings of the IEEE 23rd International Conference on Intelligent Engineering Systems*, 369–374.

Drexler, D.A., Ferenci, T., Lovrics, A., and Kovács, L. (2019b). Tumor dynamics modeling based on formal reaction kinetics. *Acta Polytechnica Hungarica*, 16(10), 31–44.

Drexler, D.A., Sápi, J., and Kovács, L. (2017). Modeling of tumor growth incorporating the effects of necrosis and the effect of bevacizumab. *Complexity*, 1–11. doi: 10.1155/2017/5985031.

Érdi, P. and Tóth, J. (1989). *Mathematical Models of Chemical Reactions. Theory and Applications of Deterministic and Stochastic Models*. Princeton University Press, Princeton, New Jersey.

Fabian Morales-Delgado, V., Francisco Gomez-Aguilar, J., Saad, K., and Escobar Jimenez, R.F. (2019). Application of the Caputo-Fabrizio and Atangana-Baleanu fractional derivatives to mathematical model of cancer chemotherapy effect. *Mathematical Methods in the Applied Sciences*, 42(4), 1167–1193. doi: 10.1002/mma.5421.

Füredi, A., Szebényi, K., Tóth, S., Cserepes, M., Hámori, L., Nagy, V., Karai, E., Vajdovich, P., Imre, T., Szabó, P., Szüts, D., Tóvári, J., and Szakács, G. (2017). Pegylated liposomal formulation of doxorubicin overcomes drug resistance in a genetically engineered mouse model of breast cancer. *Journal of Controlled Release*, 261, 287–296. doi:10.1016/j.jconrel.2017.07.010.

Ionescu, C.M. (2018). A computationally efficient Hill curve adaptation strategy during continuous monitoring of dose-effect relation in anaesthesia. *Nonlinear Dynamics*, 92(3), 843–852.

Jarrett, A.M., Lima, E.A.B.F., Hormuth, D.A., McKenna, M.T., Feng, X., Ekrut, D.A., Resende, A.C.M., Brock, A., and Yankeelov, T.E. (2018). Mathematical models of tumor cell proliferation: A review of the literature. *Expert Review of Anticancer Therapy*, 18(12), 1271–1286. doi:10.1080/14737140.2018.1527689.

Kühleitner, M., Brunner, N., Nowak, W.G., Renner-Martin, K., and Scheicher, K. (2019). Best fitting tumor growth models of the von Bertalanffy-PütterType. *BMC Cancer*, 19. doi:10.1186/s12885-019-5911-y.

Murphy, H., Jaafari, H., and Dobrovolny, H.M. (2016). Differences in predictions of ODE models of tumor growth: a cautionary example. *BMC Cancer*, 16. doi: 10.1186/s12885-016-2164-x.

Paez Chavez, J., Gurbuz, B., and Pinto, C.M.A. (2019). The effect of aggressive chemotherapy in a model for HIV/AIDS-cancer dynamics. *Communications in Nonlinear Science and Numerical Simulation*, 75, 109–120. doi:10.1016/j.cnsns.2019.03.021.

Perestyuk, N.A., Plotnikov, V.A., Samoilenko, A.M., and Skripnik, N.V. (2011). *Differential Equations with Impulse Effects, Multivalued Right-hand Sides with Discontinuities*. De Gruyter, Berlin, Boston. doi: 10.1515/9783110218176.

Tóth, J., Nagy, A.L., and Papp, D. (2018). *Reaction kinetics: exercises, programs and theorems*. Springer.